A Hydrodynamic Theory for Spatially Inhomogeneous Semiconductor Lasers: II. Numerical Results

Jianzhong Li[*] and C. Z. Ning[†]

Computational Quantum Optoelectronics
NASA Ames Research Center,
M/S T27A-1, Moffett Field, CA 94035-1000
(Dated: December 31, 2001)

We present numerical results of the diffusion coefficients (DCs) in the *coupled diffusion model* derived in the preceding paper [J. Li and C. Z. Ning, Phys. Rev. A 65] for a semiconductor quantum well. These include self and mutual DCs in the general two-component case, as well as density- and temperature-related DCs under the single-component approximation. The results are analyzed from the viewpoint of free Fermi gas theory with many-body effects incorporated. We discuss in detail the dependence of these DCs on densities and temperatures in order to identify different roles played by the free carrier contributions including carrier statistics and carrier-LO phonon scattering, and many-body corrections including bandgap renormalization and electron-hole (e-h) scattering. In the general two-component case, it is found that the self- and mutual-diffusion coefficients are determined mainly by the free carrier contributions, but with significant many-body corrections near the critical density. Carrier-LO phonon scattering is dominant at low density, but e-h scattering becomes important in determining their density dependence above the critical electron density. In the single-component case, it is found that many-body effects suppress the density coefficients but enhance the temperature coefficients. The modification is of the order of 10% and reaches a maximum of over 20% [C. Z. Ning and J. Li, Phys. Rev. B: Rapid Communications, submitted (2002)] for the density coefficients. Overall, temperature elevation enhances the diffusive capability or DCs of carriers linearly, and such an enhancement grows with density. Finally, the complete dataset of various DCs as functions of carrier densities and temperatures provides necessary ingredients for future applications of the *model* to various spatially inhomogeneous optoelectronic devices.

PACS numbers: PACS Numbers: 42.55.Px, 42.65.Sf, 78.20.Bh

I. INTRODUCTION

In the preceding theoretical paper [1], we have derived a set of *coupled diffusion equations* for the densities and temperatures of electrons and holes in a spatially inhomogeneous semiconductor quantum well (QW). Our derivation is based on a microscopic kinetic theory for the electron-hole plasma (EHP) model. Such a first-principle approach allows us to derive explicit expressions for all momentum and energy (and thus temperature) relaxation rates and for various diffusion coefficients (DCs), including the general two-component (TC) case and the single-component (SC) case under the ambipolar diffusion approximation (ADA) or in the strong electron-hole (e-h) scattering limit. The diffusion coefficients are given in terms of momentum relaxation rates, many-body corrections, and derivatives of carrier thermal energies [1]. Ultimately, the coefficients become functions of the thermodynamic variables of the EHP through these quantities. The application of the model is not restricted to lasing devices. Rather, it can be easily adapted to describe EHPs in other types of devices, such as photodetectors and photoconducting devices. Obviously, any application

of our model rely upon the knowledge of the diffusion coefficients.

The purpose of the present paper is two fold: First, we want to analyze in detail the behaviors of these DCs and understand them in terms of underlying physics processes. As we will show, all features of the DCs can be explained in terms of Fermi gas theory with the proper inclusion of many-body effects [2]. Second, we want to present a complete dataset for these DCs as functions of densities and temperatures to provide guidance for any future applications of this model to various optoelectronic devices. Since most of such applications ultimately will involve extensive simulation of the partial differential equations, it is essential to have those DCs tabulated and eventually fitted as analytical functions of densities and temperatures beforehand so that time-consuming microscopic calculations can be avoided.

For the numerical results, we choose an 8 nm $Al_{0.3}Ga_{0.7}As/GaAs$ quantum well structure as the model material system. Relevant material parameters are well-documented in the literature, and thus will not be listed here. For this structure, typical plasma density is 10^{12} cm^{-2} for room temperature lasing operation. Thus the ranges for the thermodynamic variables are chosen for densities from 10^{10} to 10^{13} cm^{-2} and for temperatures from 200 to 400 K. To manage the already very lengthy analysis, we shall not further differentiate temperatures between electrons and holes and use the term plasma temperature to denote the common temperature. As

---
*Electronic address: jianzhng@nas.nasa.gov
†Electronic address: cning@mail.arc.nasa.gov; URL: http://www.nas.nasa.gov/~cning

shown in the numerical results, temperature plays a very predictable role. Additionally, we restrict our presentation and discussions to density-related results at 300 K only for the general two-component case and discuss the temperature-related coefficients only for the SC case.

To help the discussions in the two-component case, we distinguish carrier types (electrons and holes) and their associated variables between primary and secondary ones when we present a diffusion coefficient. Such an assignment stems from the fact that the coefficient relates the gradient of the primary variable to the current of the secondary variable. For example, when the diffusion coefficient $D_{N^\alpha N^\beta}$ is discussed, where $\alpha, \beta \in \{e, h\}$, we refer to N^β as the primary carrier density, or simply primary density, and the β-carriers as primary carriers. Accordingly, N^α is referred to as the secondary carrier density, or simply secondary density, and the α-carriers as secondary carriers. As an extension to this convention, the primary type is itself for quantities with only one carrier type in the index, but they may depend on variables of the other type implicitly. The coefficient $D_{N^\alpha N^\alpha}$ and factor μ_α are such instances, which are functions of not only the primary density N^α and temperature T^α, but also the secondary density N^β and temperature T^β. Finally, in order to be consistent with this convention, for all other quantities or terms denoted by both carrier types, their primary type follows their associated DCs. For instance, for the term $H_{N^h}^\epsilon$ which appears in Eq. (6), its primary carrier type is the holes.

The paper is organized as follows. In Section II, we summarize those key results in 2D Fermi gas theory which are critical in understanding the diffusion coefficients. Then, we present and discuss the carrier momentum and temperature relaxation rates due to carrier-LO (longitudinal optical) phonon scattering and electron-hole (e-h) scattering in Section III. Density diffusion coefficients in the general two-component case are presented and analyzed in Section IV, followed by all the DCs for the two-component case in Section V. A summary is given in Section VI for the numerical results, together with concluding remarks regarding the scope and validity of the *model*, many-body effects, and a comparison with 3D results in the literature. Finally, we make an acknowledgment.

II. KEY RESULTS OF 2D FERMI GAS THEORY

Since properties of the ideal Fermi gas will be important in understanding the behavior of the momentum relation rates and all the DCs, we summarize certain key results of 2D Fermi gas theory. These results are obtained by applying the independent electron approximation [3]. Furthermore, some terms frequently referred to in the rest of the paper shall be introduced in this section.

First of all, the carrier thermal energies W^α's of the 2D EHP [cf. Eq. (D8) in Ref. 1] can be approximated at low and high density limits as follows:

$$W^\alpha = \begin{cases} N^\alpha k_B T^\alpha \,, & \text{Maxwell dist.} \\ w_0^\alpha(N^\alpha) + w_2^\alpha(N^\alpha)T^{\alpha 2} \,, & \text{Fermi-Dirac dist.} \end{cases} \quad (1)$$

where we have indicated the statistics applicable in each case. Within the limited temperature range between 200 K and 400 K interested in this paper, the statistical property or the degeneracy is determined by the density alone. While the first line of Eq. (1) is the familiar classical result of the Boltzmann statistics, the second line is obtained for the degenerate limit using the Sommerfeld expansion. The first term $w_0^\alpha(N^\alpha)$ has a quadratic density dependence, but no temperature dependence. The remaining term contributes to all the temperature dependence despite its weak dependence on density. Therefore, the free carrier thermal energy has a bilinear combination of density and temperature in the classical regime, while it is an addition of two quadratic terms of temperature and density, respectively. Thus it follows naturally that density (temperature) derivative is independent of density (temperature), while linearly dependent on temperature (density) in the classical regime. This is exactly the opposite in the quantum or degenerate regime where density (temperature) derivative depends linearly on density (temperature), while showing no dependence on temperature (density). Obviously, the energy derivatives (or specific heats) in the two regimes exhibit different behaviors. Since the DCs are closely related to such derivatives, we expect different behaviors of DCs in two regimes. The physical origin of the difference is the statistical degeneracy or Pauli's principle in the quantum regime.

Next, we will illustrate how the transition from the classical regime to the quantum regime can be quantitatively characterized, and the role played by the different masses of electrons and holes. It can be shown [see Eq. (D10) in Ref. 1] that the density derivative of the thermal energy of α-carriers is given by

$$\partial_{N^\alpha} W^\alpha = \frac{\pi \hbar^2 N^\alpha}{m_\alpha} \left[1 + \exp(-\frac{\mu_F^\alpha}{k_B T^\alpha}) \right] \,, \quad (2)$$

where μ_F^α is the chemical potential of α-carriers. The chemical potential for fermionic particles increases monotonically with their density owing to Pauli's principle. To be exact, the chemical potential depends linearly on the density in the quantum regime. In the classical regime, however, $\partial_{N^\alpha} W^\alpha = k_B T^\alpha$ because the exponential term becomes important as the chemical potential gets negatively large. Therefore, it is clearly shown from the above equation that the carrier density corresponding to zero chemical potential is an excellent quantitative indicator for the transition from the classical regime to the quantum regime. Such a density is called "the critical density" [4] in literature, despite the non-critical nature of the transition. The 2D critical density is given by

$$n_{cr}^{2D} = \frac{m_\alpha k_B T}{\pi \hbar^2} \ln 2 , \qquad (3)$$

which is about 5×10^{11} cm^{-2} for electrons and 3×10^{12} cm^{-2} for holes at room temperature. As defined, the critical density provides a quantitative measure above which statistical degeneracy for fermionic particles becomes important. As a consequence of statistical degeneracy, the phase space-filling effects greatly influence the physical properties of the Fermi gas in the quantum regime. In the quantum regime, energy for the 2D Fermi gas is in the order of chemical potential, instead of the thermal energy $k_B T$ in the classical regime. The constant density of states (DOS) in 2D leads to the linear relationship between chemical potential and density, as mentioned earlier. Therefore, the change in the energy scale, thus its characteristics, as a manifestation of the phase space-filling effects, results in corresponding behavioral transitions in the physical properties of the Fermi gas. Such transitions are ushered in at the critical density.

Now let us discuss the case of an EHP. The total thermal energy of the plasma is the sum of that of electrons and holes. As revealed by Eq. (3), because of their different masses, the lighter electrons step into the quantum regime before the holes, as we increase densities. After the transition for electrons, their contribution to the total thermal energy becomes larger than holes, as a result of the stronger density dependence. Therefore, the critical electron density masks the critical hole density, as far as density derivatives of the thermal energies are concerned. However, the story is not complete without considering temperature derivatives of the thermal energies. It is interesting to show [see equations (D.10) and (D.11) in Ref. 1] that the following relationship holds for any density and temperature:

$$N^\alpha \partial_{N^\alpha} W^\alpha + T^\alpha \partial_{T^\alpha} W^\alpha = 2W^\alpha . \qquad (4)$$

This is in fact Euler's theorem for homogeneous functions of degree 2, which states that the thermal energy is a linear superposition of quadratic polynomials in density and temperature. This equation dictates a quadratic density dependence for the term $w_0^\alpha(N^\alpha)$ and no dependence for $w_2^\alpha(N^\alpha)$ in the quantum regime. Note that these results are consistent with the results presented earlier. However, the first term dominates over the second term quantitatively, which is what the above equation fails to reveal and why electronic specific heat is much smaller in a normal metal than in an ideal gas. As such, we see immediately that the critical hole density masks the critical electron density for temperature derivatives. Nevertheless, it is important to point out that around the critical density smooth transitional behaviors are anticipated. Furthermore, as the upper density bound in the range of interest is marginally higher than the hole critical density, we expect certain degree of modification to the limiting

cases we have presented here. One of them is the density dependence of the temperature derivatives that do show density dependence above the critical density, but the dependence slowly decreases with density. Finally, it is also true that for quite a many physical quantities of the EHP, netiher the critical electron density nor the critical hole density is the proper density that characterizes the statistic transition because the EHP is a mixture of electrons and holes after all. Instead, the transparency density of the EHP, given by $\mu_F^e + \mu_F^h = 0$ and denoted by n_{tr}^{2D}, is a better representative of the transition, especially for neutral plasmas. The density has a magnitude between the critical electron density and the critical hole density, as easily seen from its definition, since the chemical potential is a monotonous function of density. In general, it is appropriate to use the critical density of the predominant carrier type for characterization of the statistic transition; otherwise, the transparency density is a better choice.

To close this section, we emphasize that the critical densities introduced here are useful for general understanding of the numerical results presented in the present article, as their existence is a mere exposure of the fermionic nature of the EHP. They will be extensively referred to later as we discuss the underlying physics of the results.

III. MOMENTUM AND TEMPERATURE RELAXATION RATES

Momentum relaxation is the underlying physics process for carrier diffusion and the various relaxation rates appear naturally in the expression of DCs as we will see in the next section . To prepare ourselves for the explanation of the diffusion coefficients, we present in this section the relaxation rates obtained microscopically in Ref. [1]. In short, the rates are treated within the second Born approximation [5]. Screening of the Coulomb interaction is described under the single plasmon pole approximation [6, 7]. Numerical integration for the rates is implemented with forty-point Gaussian quadratures after necessary simplifications. Both momentum and temperature relaxation rates are shown, even though the temperature relaxation (or the Newton's cooling) rates do not affect the DCs. The temperature relaxation rates are used in the temperature equation(s) in the *coupled diffusion model*. Two major scattering mechanisms are considered in our model: e-h and carrier-LO phonon (c-LO) scatterings.

Results for momentum relaxation rates due to e-h and c-LO phonon scattering are presented in Fig. 1. For the e-h scattering rates shown, electron and hole density are equal. At low density, the e-h scattering rate shows a linear density dependence, while the c-LO scattering rates are density independence. All the rates decrease above certain transition density which increases with temperature and is higher for holes. For the e-h scattering rate,
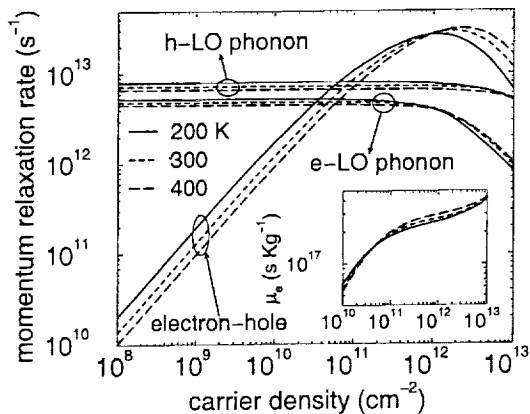
FIG. 1: Carrier momentum relaxation rates as a function of density and temperature. All the results shown in this article are for an 8 nm $Al_{0.3}Ga_{0.7}As$/GaAs quantum well. The inset shows the μ_e factor given by Eq. (31) in Ref. [1]. The electron density and hole density are identical for the electron-hole scattering and the μ_e factor here. Note that this μ_e factor is different from the one used under the single-component approximation [cf. Eq. (13)] and is not carrier mobility either.
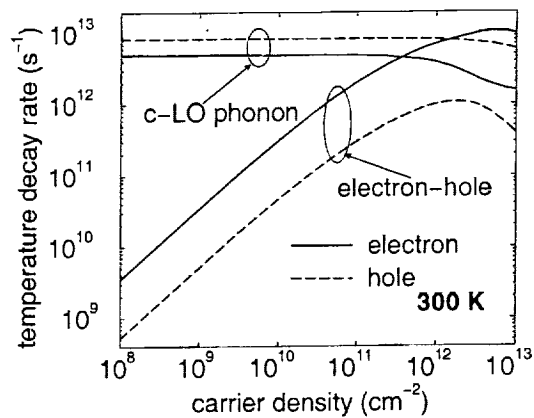
FIG. 2: Comparison of carrier temperature relaxation rates as a function of density and temperature. The results shown are obtained microscopically following Appendix A and B in Ref. [1].

the decrease starts along with the e-LO scattering rates. Overall, temperature dependence is relatively weak for all the rates. Specifically, rise in temperature reduces all the rates at low density, but the dependence is reversed above the transition density. The characteristic change for the rates across the transition density is associated with statistical leap from classical to quantum regime by the fermionic particles of the EHP. Consistently, quantitative comparison allows us to identify the density as the critical density n_{cr}^{2D} defined earlier. Furthermore, its temperature and carrier type dependence agree well with those of the critical density.

Next, we explain the overall density-dependence behaviors of the rates in light of quantum degeneracy. At low density, particles follow Maxwell distribution and behave independently. Thus the c-LO phonon scattering rates are density-independent. The e-h scattering rate, because of its binary nature, is directly proportional to the secondary density (type β), and independent of the primary density (type α). As the two densities are the same in the figure, we see the linear density dependence. In contrast, in the quantum regime, owing to Pauli's principle, phase space-filling effects start to appear. Limitation in the available phase space for out-scattered fermionic particles causes reduction in the scattering rates, and thus relaxation rates. Both carrier types are subject to the phase space-filling effects, despite starting at different critical densities. Now we examine the role of the plasma temperature. In the classical regime, increase in temperature leads to population shift to high energy or momentum states, but low momentum states are favored for relaxation processes because they transfer momentum more effectively to the

phonons. Thus the rates drop. As for e-h scattering, the same argument applies, but since both carrier types are affected by the temperature change, we see an enhancement in its temperature dependence in Fig. 1. As carriers move into the quantum regime, Pauli's principle plays a predominant role in limiting momentum relaxation. Nonetheless, rise in temperature reduces the degree of statistical degeneracy, hence enhances relaxation processes, as demonstrated by the high density results in the figure. At the same time, the temperature change also shifts the critical density to higher value. Finally, the difference in the electron and hole masses gives the higher critical density for the latter, as clearly shown in the c-LO phonon relaxation rates. The higher hole-LO phonon rates are another manifestation of the larger mass of the holes since it means more effective momentum transfer or relaxation as more low momentum states are populated by holes.

It is also interesting to note the quantitative difference between the momentum relaxation rate due to c-LO phonon scattering and the rate due to e-h scattering. According to our arguments for the limiting case of strong e-h scattering in Ref. [1], the single-component approximation for such a case is marginally justified, as the momentum relaxation rate due to e-h scattering (shown in Fig. 1) is only a few times larger than the one due to c-LO phonon scattering around the transparency density.

The Newton type of cooling due to energy exchange between electrons and holes is a pure many-body phenomena. As far as we know this rate has not been calculated microscopically in the literature. We thus present in the remaining of this section the temperature decay rates due to e-h scattering and due to c-LO scatterings in Fig. 2 in close resemblance to the momentum relaxation data. Qualitatively each decay rate follows similar behavior to its counterpart in Fig. 1, therefore, only decay rates at 300 K are shown. In addition, the same understanding

for momentum relaxation processes is applicable here. Nevertheless, we note that the cooling rates for electrons and holes due to e-h scattering are different as a result of their different masses, as also explained in Ref. [1]. This is different from the situation of momentum relaxation where there is no such a difference. The reason is that the total momenta of the EHP are conserved all the time so that the momentum relaxation rates have to be the same. However, for temperature cooling it is the total energy that is conserved. Energy conservation only demands that the same amount of energy be exchanged between electrons and holes, but their decay rates also depend on their specific heats. The difference in their specific heats of electrons and holes, owing to their different masses, explains why the cooling rates have to be different for electrons and holes. In the quantum regime, this rate difference is enlarged by the phase space-filling effects, as is seen in the high density regime of Fig. 2. As a result, the holes are much more difficult to cool down than the electrons. Regarding the c-LO cooling rates, we see that holes have a larger rate than electrons as a result of larger population (product of distribution function and the density of states) in the low energy states. Such lower energy states are favored for very effective energy transfer to phonons via the scattering, as compared to the lighter electrons. Also, the heavier holes have a higher critical density. Therefore, not only the holes have a larger cooling rate than the electrons, but also a weaker density dependence at the same time.

As we close this section and move on to the presentation of diffusion coefficients, we note that only momentum relaxation rates are involved. So, all relaxation rates are meant for momentum relaxation later unless indicated otherwise.

IV. DIFFUSION COEFFICIENTS FOR A TWO-COMPONENT PLASMA

In this section we present results for the density-related diffusion coefficients in the general two-component case as a function of electron and hole densities. For convenience, the formulation for the coefficients is collected below [1]:

$$D_{N^e N^e} = \mu_e \left[(1 + \eta_e) S^e_{N^e} + H^h_{N^e} \right] , \qquad (5)$$

$$D_{N^e N^h} = \mu_e \left[(1 + \eta_e) H^e_{N^h} + S^h_{N^h} \right] , \qquad (6)$$

$$D_{N^h N^e} = \mu_h \left[(1 + \eta_h) H^h_{N^e} + S^e_{N^e} \right] , \qquad (7)$$

$$D_{N^h N^h} = \mu_h \left[(1 + \eta_h) S^h_{N^h} + H^e_{N^h} \right] , \qquad (8)$$

where $S^\alpha_{N^\alpha} = \partial_{N^\alpha} W^\alpha + N^\alpha \partial_{N^\alpha} \delta\epsilon^\alpha$ and $H^\alpha_{N^\beta} = N^\alpha \partial_{N^\beta} \delta\epsilon^\alpha$, $(\alpha, \beta \in \{e, h\} \mid \alpha \neq \beta)$. Here W^α is the thermal energy of α-carriers and $\delta\epsilon^\alpha$ is the many-body correction to the carrier self energy of type α. We refer to $S^\alpha_{N^\alpha}$ and $H^\alpha_{N^\beta}$ as self-terms and mutual-terms, respectively.

A. A Few Important Functions of Density and Temperature

We note that DCs in Eqs. (5–8) are given in terms of three groups of factors: μ_α's, η_α's, and $\{S^\alpha_{N^\alpha}, H^\alpha_{N^\beta}\}$. It helps tremendously in the interpretation of the results for the coefficients to first analyze these quantities as functions of carrier densities and plasma temperatures. Within the EHP model, all the physical effects can be grouped into free carrier and many-body contributions. The former includes carrier statistics and c-LO phonon scattering, while the latter includes many-body corrections to the carrier self energy and the e-h scattering. The many-body corrections appear in the form of bandgap renormalization (BGR) in the high density case. Note that statistical degeneracy is a kind of carrier correlation and is regarded as free carrier contribution, since its origin is of statistical nature, rather than the Coulomb-mediated carrier-carrier interaction.

We first examine factor μ_α, as defined by Eq. (31) in Ref. [1]. Results for the case of equal electron and hole density are shown as an inset in Fig. 1. The main feature of the curves are the linear density dependence at low density, and a generally weak dependence otherwise. It decreases with temperature at low density, but increases at high density. Apparently, its linear density dependence originates from the secondary density dependence of the e-h scattering rate. As will be explained later, this linear density dependence results in a similar secondary density dependence at low density for mutual-diffusion coefficients.

Next, we take a close look at factor η_α which is given by $\gamma^\beta_{LO}(m_e + m_h)/\gamma^\beta_{eh} m_\alpha$. Thus it is essentially the ratio of the c-LO phonon scattering rate to that of e-h scattering. This factor, as can be inferred from Fig. 1, has an inverse linear relationship with the primary density N^α, but is independent of the secondary density N^β at low density. The relationship is weaker than, but close to, linear on both densities at high density. In particular, it has a V-shaped minimum near the critical primary density. The consequent effects on the self-diffusion coefficients will be identified in more detail in the next subsection, but an a qualitative examination of Eqs. (5) and (8) allows us to anticipate the main feature. Furthermore, the magnitude of η_α is in the hundreds at low density and in the order of one near the critical density. So it acts as a magnification factor for the originally weak many-body corrections, which is also obvious by inspecting Eqs. (6) and (7). In addition, η_e is order of magnitude larger than η_h because of both the lighter mass of the electrons and larger h-LO phonon scattering rate. Both factors μ_α and η_α produce most of the density dependence for all the coefficients at low density, and further lead to superlinear behavior of the coefficients at high density by adding to the linear density dependence due to the free carrier contributions. However, the product of these two factor yields no density dependence at low density. Incidently, this product is related to the carrier mobilities.

The last group of functions are $S_{N^\alpha}^\alpha$ and $H_{N^\alpha}^\beta$. $S_{N^\alpha}^\alpha$'s are normally orders of magnitude greater than $H_{N^\alpha}^\beta$'s, but this margin can be greatly reduced near the critical density. In the extreme case, the margin is merely 50 percent at the critical hole density when the electron density is high enough. The self-terms contain a dominant free carrier part $(\partial_{N^\alpha} W^\alpha)$ and a negative BGR part $(N^\alpha \partial_{N^\alpha} \delta\epsilon^\alpha)$, while the mutual-terms consist only of a BGR part $(N^\alpha \partial_{N^\beta} \delta\epsilon^\alpha)$. As the free carrier part has been fully accounted for in Section II, we focus upon the BGR parts here. Due to the attractive nature of the Coulomb interaction between electrons and holes, the BGR self-energy itself is negative. Both the screening effect and the BGR parts deminish at low density, while the former increases with both densities in the density range shown. Furthermore, despite the absence of the so-called Coulomb hole (CH) correlation in the electron self-energy, electrons' BGR part in the self-terms behaves similarly to their hole counterpart. Specifically, the part is negative and increses with the primary density but decreases with the secondary density in the density range shown. In stark contrast, the situation is different for the mutual-terms, which only exist thanks to the screening effect by the secondary carriers. It turns out that the presence of the large CH self-energy dictates that, below the critical hole density, the hole mutual-term $H_{N^e}^h = N^h \partial_{N^e} \delta\epsilon^h$ be negative, and the electron mutual-term $H_{N^h}^e$ be positive. The grave consequence of this difference is, as will be shown in the following subsections, that $H_{N^h}^e$ has an appreciable impact on the hole density coefficients $D_{N^e N^h}$ and $D_{N^h N^h}$, as compared to the negligible role played by $H_{N^e}^h$ on the electron density coefficients $D_{N^e N^e}$ and $D_{N^h N^e}$. The physical reasons are several fold: first and foremost, the free carrier part $\partial_{N^\alpha} W^\alpha$ plays a dominant role at lower density for electrons owing to their lower critical density than for holes. Second, the BGR contributions to the electron density coefficients are either smaller than their counterparts to the hole density coefficients or overwhelmed by the free carrier part because of the first reason. Last but not the least, the order of magnitude larger magnification factor η_e takes effect.

Concerning the density and temperature dependence of the self- and mutual-terms, we consider independently the free carrier part and the BGR part. The free carrier part relies only on the primary density and temperature. It is density independent and linearly proportional to the temperature in the classical regime. Furthermore, it is linearly dependent on the density and temperature in the quantum regime. The BGR part partially cancels the free carrier part near the critical density in the self-terms. However, the mutual-terms add to the self-terms. Because of large CH contribution, the hole-related BGR part in the self-terms has a much larger impact than the electron-related part. Thus many-body corrections influence the hole density coefficients much more than the electron density coefficients.

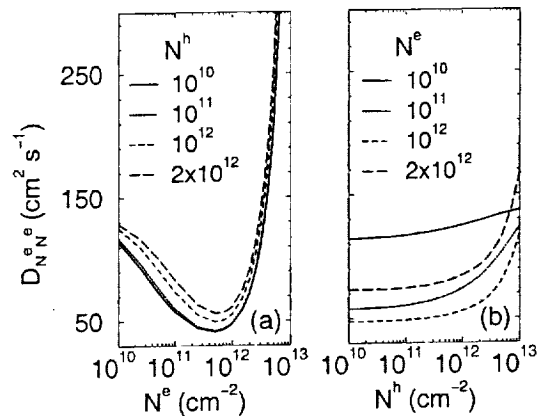In connection with the detailed analysis of the above

FIG. 3: General two-component electron-hole plasma case: self-diffusion electron density coefficient $D_{N^e N^e}$ versus electron density (Panel a) and hole density (Panel b). All data shown in Figs. 3 and 4 are at 300 K including many-body corrections.

important factors, we conclude this subsection with a summary of their impact on the diffusion coefficients in the general two-component case as follows: *The self- and mutual-diffusion coefficients are determined mainly by the free carrier contributions, but with appreciable many-body corrections near the critical density for the hole density coefficients. Carrier-LO phonon scattering is dominant at low density, but electron-hole scattering becomes important in determining their density dependence above the critical electron density. As a result, the self-diffusion coefficients are density-independent at low density, and become superlinearly dependent on the primary density. The mutual-diffusion coefficients depend linearly on the secondary density at low density. They become strongly dependent on the electron density, but weaker on the hole density than on the electron density above the critical electron density. All the coefficients depend weakly on the secondary density except $D_{N^e N^h}$. Besides, hole density coefficients are greatly modified around the critical hole density by many-body corrections.*

B. Self-Diffusion Coefficients: $D_{N^e N^e}$ and $D_{N^h N^h}$

Now we are ready for the presentation of the diffusion coefficients in the general two-component case. We show results for plasma temperature of 300 K only. In general, increase in plasma temperature leads to enhancement of diffusive capability of carriers, as will be seen in Section V for the results in the single-component case.

Depicted in Figs. 3 and 4 are the numerical results for the self-diffusion coefficients $D_{N^\alpha N^\alpha}$ with $\alpha = e, h$, respectively, where Panel (a) and (b) show the dependence of the coefficients on electron and hole densities, respectively. At low density, the coefficients decrease sublinearly with the primary density [Figs. 3(a) and 4(b)], but grow very slowly with the secondary density [Figs.
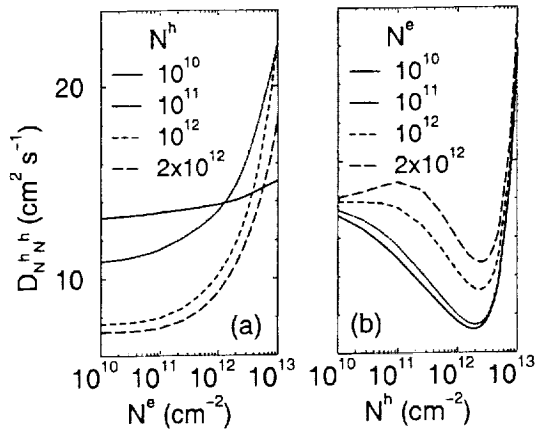
FIG. 4: General two-component electron-hole plasma case: self-diffusion hole density coefficient $D_{N^h N^h}$ versus electron density (Panel a) and hole density (Panel b).

3(b) and 4(a)]. The dependence on the primary density, however, becomes positive and superlinear at high density. Though the dependence on the secondary density increases, but it is weaker than the primary density dependence above the critical primary density. Near the critical density, the coefficients decrease by as much as 50%, thus forming the valley structures in Figs. 3(a) and 4(b). The overall behavior is comprehensible by recalling our discussions of the important functions in the last subsection. Density independence in the classical regime is expected because the free carrier part is dominant and independent of density. In addition, factor η_α is in the hundreds and its density dependence cancels that of μ_α when the two are multiplied. Carrier diffusion in this regime is dominated by the c-LO phonon scattering process, no dependence on either carrier density should be expected as a result. This picture is, however, true only at very low density and could not explain the valley structure shown in Figs. 3 and 4.

The valley stucture shown in these figures is an indication that the simple Fermi gas picture either in the classical or quantum limit is not enough to explain the behaviors of the diffusion coefficients. There are two reasons: First, a large portion of density range around the critical density in these figures falls in the intermediate regime between the two extreme limits. Second, many-body effects become important in this regime. As seen in the inset of Fig. 1, factor μ_α starts to deviate from the familiar linear density dependence of the ideal gas theory at density of about 5×10^{10} and the dependence become much weaker thereafter. At the same time, other factors also start to show deviation from their classical limits. For instance, the e-h scattering rate at 300 K is 34% lower than its expected value from a linear dependence at the density of 10^{11} cm^{-2}, as shown in Fig. 1. Therefore, the phase space-filling effects becomes appreciable before the critical density is reached. Owing to the smaller mass of electrons, such deviations appear at

lower density for them than for holes, and in larger magnitude as well. In addition, many-body effects also affect the behaviors of the coefficients, especially around the critical density. In fact, not only the BGR terms become important as carrier density increases, but also e-h scattering introduces density dependence through factors μ_α and η_α. As discussed above, the negative BGR part in the self-terms, i.e., $H^\alpha_{N\alpha}$, partially cancels the free carrier part, and thus suppress diffusive processes. As we said earlier, many-body effects in this paper contain two parts: the BGR part and the e-h scattering part. It is interesting to see how each part plays different roles in forming the valley structure in the two self-diffusion coefficients. A direct comparison of the coefficients with and without the BGR contributions reveals that the minimal structure for $D_{N^h N^h}$ is mainly due to the BGR contribution in the corresponding self-term, while it is the e-h scattering that yields the similar structure in $D_{N^e N^e}$. This means that the suppression of carrier diffusion can be due to either the attractive Coulomb interaction so that carriers tend to cluster rather than disperse apart, or increase in the e-h scattering rate so that carriers spend more time bouncing around internally rather than wandering away. The more frequent collisions for holes with LO phonons at low density mean less diffusive capability or a smaller DC for them. Consequently, e-h scattering influences the diffusive capability of electrons more than that of holes. Therefore, the reduction in the diffusive capability of electrons is mainly due to enhancement of e-h scattering as carrier density increases, and BGR contribution is responsible for such suppression in the diffusivity of holes.

It is relatively straightforward to understand the results at high density. Free carrier contributions to the self-terms have a linear primary density dependence and no dependence on the secondary density. Additionally, they are predominant over the BGR parts. As a result of the combined effects of factors μ_α, η_α, and the self-terms, the coefficients increase superlinearly with the primary carrier density [cf. Figs. 3(a) and 4(b)], but more weakly on the secondary carrier density [cf. Figs. 3(b) and 4(a)].

C. Mutual-Diffusion Coefficients: $D_{N^e N^h}$ and $D_{N^h N^e}$

The mutual-diffusion coefficients $D_{N^\alpha N^\beta}$ with $\alpha, \beta \in \{e, h\} \mid \alpha \neq \beta$ are shown in Figs. 5 and 6, respectively. Panels (a) and (b) depict the dependence of the coefficients on electron and hole densities, respectively. According to Figs. 5(a) and 6(b), these coefficients decrease and go to zero as the secondary density decreases to zero. They are independent of the primary density at low density [Figs. 5(b) and 6(a)]. At high density, they feature a superlinear growth with the electron density, but a much weaker one with the hole density. For $D_{N^e N^h}$, similar valley structure appears for high electron densities [Fig. 5(b)], but the bottom of the valley appears at a higher
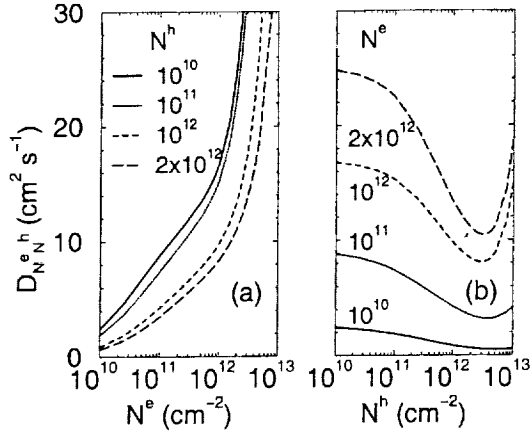
FIG. 5: General two-component electron-hole plasma case: mutual-diffusion hole density coefficient $D_{N^eN^h}$ versus electron density (Panel a) and hole density (Panel b).
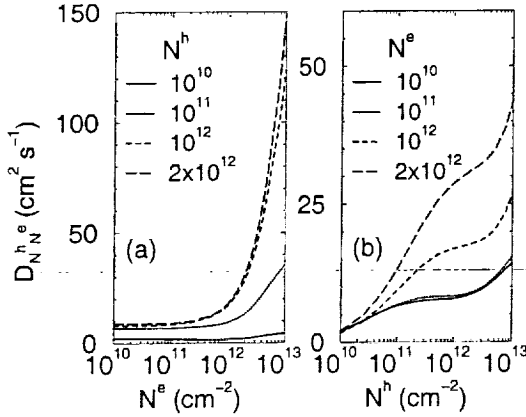

FIG. 6: General two-component electron-hole plasma case: mutual-diffusion electron density coefficient $D_{N^hN^e}$ versus electron density (Panel a) and hole density (Panel b).

density than for $D_{N^hN^h}$ [Fig. 4(b)] around the critical hole density. For $D_{N^hN^e}$, by contrast, no appreciable feature shows up around the critical electron density [Fig. 6(a)], as compared to $D_{N^eN^e}$ [Fig. 3(a)]. Finally, on secondary density dependence, a more pronounced slowdown of the transitional growth in the coefficients is observed for $D_{N^hN^e}$ near the critical hole density in Fig. 6(b) than for $D_{N^eN^h}$ near the critical electron density in Fig. 5(a).

These behaviors can be understood similarly as for the self-diffusion efficients in terms of the several factors discussed in Subsection IV A, as plainly indicated by Eqs. (5–8). We start with low density results. In this regime, the free carrier contributions have no density dependence and the BGR terms diminish such that the coefficients are well described by $D_{N^\alpha N^\beta} \approx \mu_\alpha S_{N^\beta}^\beta$. As such, the coefficients inherit the secondary density dependence of factor μ_α, or a linear dependence (Fig. 1 inset). At the same time, the coefficients have no dependence on the primary

density. Nevertheless, deviations exist due to the same reasons as discussed in the preceding subsection. After comparing with results without BGR contributions, it is found that the mutual-term $H_{N^h}^e$ approximately doubles $D_{N^eN^h}$ when the electron density is above its critical value [Fig. 5(b)]. The enhancement is attributed to factor η_e whose value is about 400 at 10^{10} cm^{-2}—that is why we call it a magnification factor. Physically, it is easy to understand these behaviors of the coefficients. Mutual diffusion process is a consequence of interactions between different types of carriers. The interactions result in both many-body corrections to the self-energy of the involving carriers and incoherent scattering events between them. It is trivially expected that the effects of the interactions on carriers of the secondary type vanish if secondary density becomes too small in the electron-hole plasma model [8]. This induced diffusive process is elevated as secondary density increases, though increase in primary density impedes such an enhancement by introducing stronger scattering and more negative many-body corrections. As carrier densities are around their critical densities, quantitative differences in the factors discussed in Subsection IV A between electrons and holes take effect. As a result, many-body corrections have a much more noticeable impact on $D_{N^eN^h}$ than on $D_{N^hN^e}$. One indication is in Fig. 5(b) where the hole density dependence features a remarkable dip near the critical density for $D_{N^eN^h}$. This behavior is because the positive BGR contribution to the mutual-term doubles the coefficients at low density through the magnification factor, in conjunction with partial cancellation of the free carrier contribution by the negative BGR part in the self-term [cf. Eq. (6)]. The cancellation is most pronounced near the critical density. For $D_{N^hN^e}$, the free electron contribution overwhelms the BGR term as the larger but negative BGR contribution to the mutual-term is partially offset by the order of magnitude smaller magnification factor η_h. As a matter of fact, factor η_h takes a value of 1 as compared to a value of 10 for η_e when both electron and hole density are 10^{12} cm^{-2}. As such, the many-body corrections bring about the minimal structure in $D_{N^eN^h}$. However, many-body correction does cause a more distinguishable slowdown in its transition into the quantum regime for $D_{N^hN^e}$ near the critical hole density, as shown in Fig. 6(b). Finally, above the critical densities, free carrier contributions take over and superlinear growth takes hold for the coefficients. However, in comparison with the self-diffusion coefficients, the density dependence of the mutual-diffusion coefficients is much weaker because of displacement of the magnification factor η_α from the self-terms to the mutual terms, as shown in Eqs. (5–8).

In summary, mutual-diffusion coefficients describe the induced diffusive capability of the secondary carriers by interacting with the primary carriers. As a result, the coefficients go to zero with the secondary densities. In addition, many-body corrections have more pronounced effects in these coefficients, especially in $D_{N^eN^h}$.

V. THE AMBIPOLAR DIFFUSION COEFFICIENTS

In this section, we present numerical results for all four ambipolar diffusion coefficients and analyze their dependence on plasma density and temperature, as well as the effects of the many-body corrections on them. For convenience, we choose the word "ambipolar" to represent the results for generic single-component cases in this article without further implication. Under the single-component approximation, the EHP is neutral and all thermodynamic properties are characterized by the plasma density and temperature. For easy reference and discussions, the expressions for the coefficients are rewritten below:

$$D_{NN} = \mu \left(\partial_N W + N \partial_N \delta\epsilon_g \right) , \qquad (9)$$

$$D_{NT} = \mu \left(\partial_T W + N \partial_T \delta\epsilon_g \right) , \qquad (10)$$

$$D_{TN} = \left[2 j_W (W/N) - j_N \right] D_{NN} , \qquad (11)$$

$$D_{TT} = \left[2 j_W (W/N) - j_N \right] D_{NT} , \qquad (12)$$

where W is the total thermal energy of the EHP and $\delta\epsilon_g = \delta\epsilon^e + \delta\epsilon^h$ is the total BGR energy. Furthermore, we have

$$\mu = 1/ \left(m_e \gamma_{LO}^e + m_h \gamma_{LO}^h \right) , \qquad (13)$$

where j_W and j_N are transformation Jacobians and given in Ref. [1]. We point out that the e-h scattering rate drops out in the present case. The absence of e-h scattering in the ambipolar mobility was noted in Ref. [9]. Consequently we see that all the ambipolar diffusion coefficients are independent of the scattering. As in the general two-component case, we start by analyzing the contributing factors to the DCs in terms of their dependence on the thermodynamic variables of the EHP, followed by presentation of the results for the DCs themselves and the associated many-body effects.

A. Density and Temperature Dependence of the Contributing Factors

As shown in Eqs. (9–12), there are four contributions to the diffusion coefficients from: (1) incoherent scattering in factor μ, (2) free carrier part represented by the derivatives of the total thermal energy W, (3) coherent many-body part represented by the derivatives of the BGR $\delta\epsilon_g$, and (4) the prefactor in the expressions of D_{TN} and D_{TT} in Eqs. (11, 12). The first three contributions have been elaborated somewhat in the two-component case in Subsection IV A. In the following, we point out their ramifications in the singe-component case and focus on the BGR contributions instead. A summary of many-body effects is presented elsewhere [10].

To begin with, we note that factor μ [cf. Eq. (13)] is independent of plasma density in the classical regime, and has a sublinear density dependence above the critical hole density owing to the dominance of the h-LO phonon scattering rate. The factor increases weakly with plasma temperature at low density, and becomes even more insensitive to temperature at high density thanks to the mixed contributions from the c-LO phonon scattering rates. Second, the free carrier part, as in the two-component case, dominates over the BGR part. In the classical regime, the free carrier contribution yields no density and linear temperature dependence for density diffusion coefficients, and no temperature but linear density dependence for temperature diffusion coefficients. In the quantum regime, it gives rise to a linear density and no temperature dependence for density diffusion coefficients, and linear temperature but no density dependence for temperature diffusion coefficients. Furthermore, the density derivative of the thermal energy $\partial_N W$ follows the critical density of the electrons, in contrast to the temperature derivative of the thermal energy $\partial_T W$, which follows that of the heavier holes when the EHP transits from the classical to quantum regime. As explained in Subsection IV A, lighter electrons enter the quantum regime at a smaller critical density than holes. In the new regime, the contribution to the total thermal energy from electrons is enhanced because the electronic energy scale, which is now the chemical potential, increases with density. However, the enhanced contribution, has a weaker temperature dependence. Consequently, free carrier contributions show different critical densities in density and temperature diffusion coefficients. Third, we discuss the BGR parts in Eqs. (9–12). In comparison with the general two-component case, the e-h scattering rate and mutual-terms drop out. The BGR parts in the self-terms are the only remaining many-body contributions. Therefore, in general, many-body effects have a less drastic impact in the present case because of the missing contributions and the dominant free carrier contributions from the electrons in the EHP. Since the value of the BGR is negative and increases with carrier density [11–13], its derivative with respect to density, $N\partial_N \delta\epsilon_g$ as appeared in Eqs. (9, 11), is negative. The magnitude of the term grows with density and saturates at high density, but is insensitive to change in temperature, However, since increase in temperature reduces the magnitude of the BGR [14], the temperature derivative $\partial_T \delta\epsilon_g$ is positive. The magnitude of the term increases superlinearly with density at low density and tends to saturate at high density. The term is insensitive to temperature. Overall, the many-body effects are relatively weakened by temperature since the free carrier contributions become more influential with an increase in temperature. Finally, the prefactor $2 j_W (W/N) - j_N$ turns out to follow approximately an inversely linear dependence on the density and increase with plasma temperature in the whole covered range, which can be easily verified by recalling that the Jacobians are defined by $j_W = 1/\partial_T W$ and $j_N = \partial_N W/\partial_T W$ and using Eq. (1).
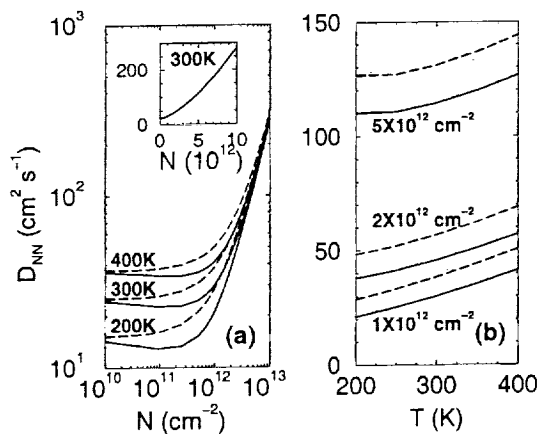
FIG. 7: The electron-hole plasma under single-component approximation case: self-diffusion density coefficient D_{NN} versus plasma density (Panel a) and temperature (Panel b). Solid lines include many-body corrections to the free carrier results (dashed lines), and the same notation is also used in Figs. 8-10. The inset shows the 300 K data with many-body effects in linear X-Y scale.

B. Self-Diffusion Density Coefficient: D_{NN}

Figure 7 shows the self-diffusion coefficient D_{NN} as a function of plasma density (a) and temperature (b). Solid and dashed curves in the figures represent results with and without the BGR terms, respectively. The self-diffusion density coefficient D_{NN} displays a superlinear density dependence at high density, and almost a constant at low density, as shown in Fig. 7(a). The transition in the density dependence occurs at the critical electron density and shifts toward higher density with temperature. The temperature dependence is linear at low density, but somewhat nonlinear at high density as shown in Fig. 7(b). These behaviors are mainly attributed to the free carrier part $\partial_N W$ in Eq. (9). As discussed earlier, factor μ is essentially density insensitive in the whole covered range. The BGR term brings some correction to the free carrier term, but does not change the basic behavior of the coefficient, which will be discussed next. It is the free carrier part that is responsible for the basic behavior of the coefficient. In particular, the dominant part increases from the classical value of $2k_B T$ to a value of the order of the chemical potential of electrons as the EHP transits from the classical into the quantum regime. Thus the coefficient D_{NN} has no density dependence and linear temperature dependence at low density. In the intermediate density range, as the lighter electrons lead holes in the transition, the transition density in Fig. 7(a) coincides with the critical electron density, and it increases with temperature, as indicated in Eq. (3). In the quantum regime, the chemical potential of electrons is approximately given by $\pi\hbar^2 N/m_e$. Therefore, these properties of the free carrier part, together with factor μ, produce the superlinear density dependence and nonlin-

ear temperature dependence of D_{NN} at high density. We remark that the drastic increase in the coefficient near the critical density is not due to the weakening in scattering. As noted, factor μ solely conveys the effects of scattering. It is clearly shown in Eq. (13) and Fig. 1 that the h-LO phonon scattering plays a dominant role. Since the scattering is basically density-independent in the covered range, we conclude that scattering is not responsible for the observed strong enhancement. Instead, the enhancement comes directly from a density-dependent gain in energy as a result of the statistical transition. As a matter of fact, such a gain appears as a prefactor in Landsberg's generalized Einstein relation [15]. Lastly, we mention that in the classical regime, the Einstein relation is recovered as $D_{NN} = 2k_B T\mu$. However, in the quantum regime the relation is modified not only by the phase space-filling effects [15], as just mentioned, but also by the many-body corrections.

Next, we discuss many-body effects on the coefficient D_{NN}. The effects stem from the BGR term $N\partial_N \delta\epsilon_g$ in Eq. (9). They result in the difference in Fig. 7 between the solid curves which include the BGR term and the dashed curves without the BGR term. As seen, the BGR term increases in size with density at low density and reaches maximum near the critical electron density. Then it decreases at high density. Temperature has no appreciable effect on the BGR contribution (difference between solid and dashed curves) as best seen in Panel (b) which is plotted in linear X-Y scale. The reduction in the coefficient by many-body effects is expected because carriers tend to congregate instead of diffuse due to the attractive nature of Coulomb interaction between electrons and holes. Thus their diffusivity or diffusion coefficient is reduced as compared to the interaction-free case. Further reduction results as interaction energy increases in magnitude with density. On the contrary, increase in plasma temperature enhances thermal motion of the EHP such that the significance of the interaction for the plasma is reduced. As a result, the effects are relatively weakened. The difference introduced by many-body effects is between 10~20%.

C. Mutual-Diffusion Temperature Coefficient: D_{NT}

The results for the mutual-diffusion temperature coefficient D_{NT} are shown in Fig. 8 in linear X-Y scale in the main Panels (a) for density dependence and (b) for temperature dependence. Additionally, the 300 K data with BGR contribution are plotted in log-log scale as an inset for comparison. At low density, the coefficient depends on the density linearly but not on the temperature. At high density, its density dependence is sublinear [Fig. 8(a)], while the temperature dependence is linear [Fig. 8(b)]. It is noted from Panel (a) and the inset that the statistical transition is characterized by the critical hole density. In the classical regime, the linear density-dependent and temperature-independent behavior is ex-
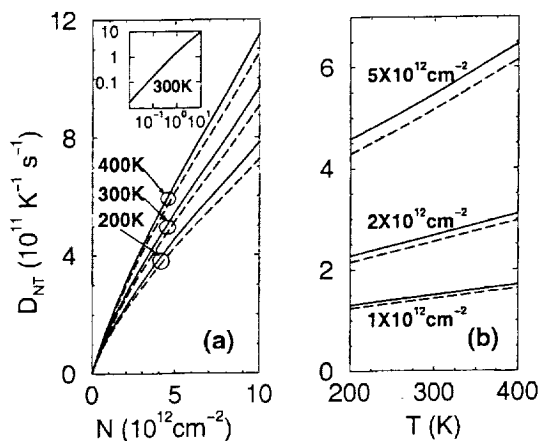
FIG. 8: The electron-hole plasma under single-component approximation case: mutual-diffusion temperature coefficient D_{NT} versus plasma density (a) and temperature (b). Linear X-Y scale is used in order to show the weak temperature dependence. The inset shows the 300 K data in a log-log scale for comparison.
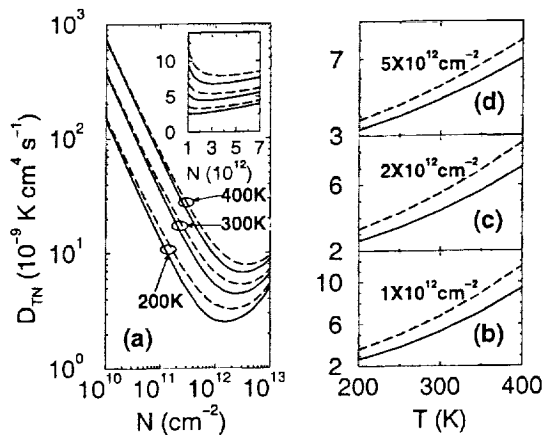
FIG. 9: The electron-hole plasma under single-component approximation case: mutual-diffusion density coefficient D_{TN} versus plasma density (a) and temperature (b-d). The inset shows the same data in linear X-Y scale for comparison. Multiple panels (b-d) are used to better illustrate the temperature dependence of the coefficient, as in Fig. 10.

pected because the dominating free carrier term demands so, while factor μ has only minor influence on the temperature dependence. In the quantum regime, the dominating free carrier part produces a linear temperature dependence but no density dependence. The sublinear density dependence comes from factor μ, as discussed in Subsection V A. As we recall, both the free carrier part $\partial_T W$ and factor μ follow the critical hole density as they enter the quantum regime, which account for the observed transition density. The overall behavior of the coefficient fits perfectly to our general understanding of the physics involved. First of all, due to its induced nature, mutual diffusion vanishes with the secondary variable. The linear density dependence at low density manifests this consistency. Second, as carriers become statistically degenerate, the induced current is reduced as a result of the limitation to available phase space. In the present case, thermal excitation of carriers is restrictive compared to classical case, which leads to smaller diffusivity. Then temperature elevation tends to lift this restriction and recover the classical result, thus we see an increase in the coefficient (cf. Fig. 8). Therefore, the main features for the coefficient D_{NT} is readily comprehended.

The many-body effects on the coefficient are reflected by the difference between the solid curves and the dashed curves. As seen, the many-body effects increase the coefficient and the amount grows with density in the density range shown. The effects are independent of temperature. From the numerical point of view, the coefficient is influenced by the BGR term $N\partial_T\delta\epsilon_g$, which is positive in the covered range, as explained in Subsection V A. In addition, the BGR term increases superlinearly with density and is weakly dependent on temperature. Thus many-body effects on the coefficient behaves exactly as expected. In comparison, the many-body effects on the

present coefficient are less than that on the self-diffusion density coefficient. The effects are understood in the following way. Recall that the present coefficient represents the induced contribution by temperature difference to the density current. The diffusive current flows from high temperature region to low temperature region. As the potential energy due to Coulomb interaction is lower in the low temperature region, force is thus induced by the temperature difference and this force helps current flow. Therefore, many-body effects contribute positively to the coefficient. The potential energy increases with density in magnitude. The growth is superlinear at low density and becomes slower at high density because phase space-filling effects take effect. Therefore, the enhancement of the coefficient by many-body effects behaves the way physics dictates. Finally, it is worth noting that, as indicated by Eqs. (9–12), the two remaining DCs are affected by many-body effects in the same manner as the two we just showed, so the effects shall not be further discussed. In summary, many-body effects reduce the density coefficients but enhance temperature coefficients. Plasma temperature has negligible influence over the effects on all the coefficients.

D. Mutual-Diffusion Density Coefficient: D_{TN}

In this subsection, we present the results for the mutual-diffusion density coefficient D_{TN} as shown in Figure 9. Density and temperature dependence of the coefficient are plotted in Panel (a) and (b-d), respectively. In the inset of Panel (a), the same data from the panel are presented in linear X-Y scale for comparison.

The coefficient decreases linearly at low density and increases sublinearly at high density. The transition oc-

curs at a higher concentration than for D_{NN} and seemingly follows the critical hole density. The temperature dependence shows stronger than linear behavior. Understanding these results is straightforward by looking at Eq. (11) and keeping in mind how the prefactor behaves as discussed in Subsection V A. The prefactor depends inversely on density but linearly on temperature, which translates into an inverse proportionality of the coefficient to density at low density and sublinear dependence at high density. The prefactor masks the critical electron density by shifting the transition density to a higher value than for D_{NN}, and further transforms the high density behavior of D_{TN} from the superlinear dependence of D_{NN} to the present sublinear dependence as exhibited in Fig. 9(a). On the other hand, the temperature dependence of D_{TN}, as seen in Fig. 9(b–d), becomes stronger than that of D_{NN}, as enhanced by the factor. Now we examine the results from the physical perspective. The present coefficient measures the temperature diffusivity induced by density difference. First, it vanishes with the secondary variable, i.e., plasma temperature, at low temperature, as expected and indicated in Fig. 9(b–d). Second, at low density, thermal energy current flows in proportion with density gradient as energy scales linearly with density. However, temperature, as an intensive quantity, does not scale with density. Thus the induced temperature diffusivity scales inversely with density. As phase space-filling effects set in as density increases, the diffusivity is enhanced because increased energy amount at the same temperature as compared to the classical case, which is revealed in Panel (a). Then temperature elevation hoists energy amount at any given density, which improves the mutual diffusion in the whole range shown.

E. Self-Diffusion Temperature Coefficient: D_{TT}

We present the results for the self-diffusion temperature coefficient D_{TT} in this subsection in the same manner used for D_{TN}. As shown in Fig. 10, the coefficient shows positive but quite weak dependence on density at low density and sublinear decrease above the critical hole density. A slightly superlinear temperature dependence is shown by the coefficient. Similar to D_{TN}, the behavior of the coefficient can be numerically understood starting from the prefactor and D_{NT}, as plainly told by Eq. (12). Therefore, we shall omit discussions from the numerical viewpoint, but to focus on the physical comprehension of the results. To start, we state that the self diffusion of temperature is associated with the thermal energy of the carriers. This is the fundamental reason why the two self-diffusion coefficients D_{NN} and D_{TT} share similar values in the classical regime, as shown in Figs. 7 and 10. The thermal energy is linearly proportional to density and temperature at low density, which lead to the well known Wiedemann-Franz law [3]. Hence the self temperature diffusion correlates with self density
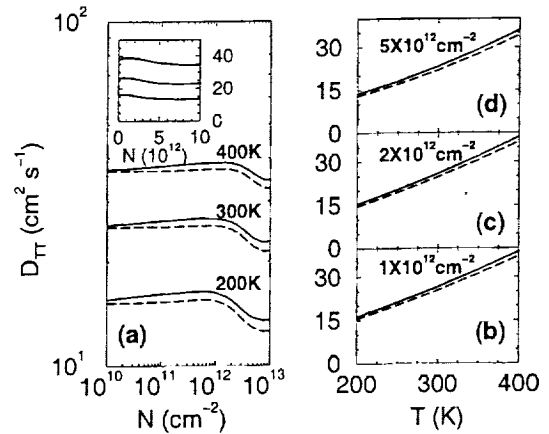

FIG. 10: The electron-hole plasma under single-component approximation case: self-diffusion temperature coefficient D_{TT} versus plasma density (a) and temperature (b). The inset shows the many-body corrections-included data in linear X-Y scale for comparison.

diffusion, which results in quantitatively similar behaviors between the self-diffusion coefficients. However, in the quantum regime, statistical degeneracy completely breaks down the bilinear dependence of the energy on density and temperature. The self-diffusion density coefficient is drastically enhanced as a result of reduced scattering rates because of the phase space-filling effects. But reduction in scattering rates does not help self-diffusion temperature coefficient. On the contrary, less scattering means less thermal motion as if the temperature were lower. Therefore, we see how physically the coefficient decreases with density in the quantum regime. The effect of temperature elevation is comprehensible in similar manner as to the other coefficients discussed earlier, and thus ignored.

In summary, it has been shown for the diffusion coefficients in the single-component approximation that many-body effects suppress the density coefficients but enhance the temperature coefficients. The modification is of the order of 10% and reaches a maximum of over 20% [10] for the density coefficients and keeps growing for the temperature coefficients in the parameter range shown. However, the many-body effects play a minor role in determining the dependence of the coefficients on plasma density and temperature. The free carrier contributions are dominantly responsible for such dependence of the coefficients. In the classical regime, the self-diffusion coefficients have no density dependence. However, the density coefficient is enhanced to a superlinear dependence, while the temperature coefficient is reduced sublinearly, as a result of statistic degeneracy in the quantum regime. By contrast, the mutual-diffusion coefficients behave distinctly differently. The temperature coefficient vanishes linearly with the density in the classical regime, but the density coefficient scales inversely with density. Nevertheless, in the quantum regime, both of them scale sub-

linearly with density. Overall, temperature elevation enhances the diffusive capability or diffusion coefficients of carriers linearly, and such an enhancement grows with density.

VI. SUMMARY AND CONCLUDING REMARKS

In this section, we make a few general comments on certain aspects of our *coupled diffusion model* and the numerical results presented in the preceding sections. By doing so, we shall achieve a better physical understanding of the present hydrodynamic description of transport of the EHP in a quasi-two-dimensional QW structure.

First of all, it is realized that a general treatment of carrier transport at low density on hydrodynamic level is hindered by Coulomb interaction between electrons and holes. Sophisticated theoretical work exists on such exciton-plasma systems for moderately low density and pure excitonic systems at lower density [16, 17], but state-of-the-art laser models fail to include such complexity. In this regard, our *coupled diffusion model* represents an effort towards incorporating such physical complexity. This is the premise upon which we justify our low density results. As such, we call the low density range below the critical densities the classical regime. Furthermore, the terminology implies a classical statistical treatment and an extension of many-body theoretical results which includes the BGR contributions and scattering rates in this range.

Next, we make some observations on the many-body effects on the diffusion coefficients. As seen in Ref. [1], it is clear that BGR contributions and e-h scattering play drastically different roles in the general TC case than in the SC case. Nevertheless, the results are self-consistent, which is expected since the single-component case is just a limiting case of the general two-component one. If the electron-hole pair in the EHP is treated as a single entity, as being done under the single-component approximation, the incoherent e-h scattering drops out and has no influence on plasma transport. However, the BGR contributions do have an effect on all the DCs, even though the size of the effect varies from coefficient to coefficient.

Now we make a comparison between the self-diffusion density coefficient D_{NN} in our quasi-2D case and its counterpart in 3D case under the ADA approximation. The coefficient for bulk GaAs was calculated and presented as Fig. 7 (solid ambipolar curve in the lower panel) in Ref. [18] as a function of plasma density. The result is compared to our quasi-2D results in Fig. 9(a). Similar transition of the density dependence from the classical to the quantum regime is observed in 3D case, and our coefficient is marginally larger than the bulk value in the density range shown. The transitional behavior in our quasi-2D case is found to occur at a smaller density than in 3D case after converting 2D density to 3D. To understand this difference, we reiterate that the transi-

tion occurs because of statistical degeneracy in the quantum regime. As carriers become degenerate, their energy scale becomes the chemical potential instead of the thermal energy scale $k_B T$ in the classical regime. Needless to say, the classical energy scale is density-independent. The chemical potential in the quantum regime is mainly determined by density, but its value differs in different dimensions because of different DOS. Therefore, physical quantities of an EHP in different dimensions have different values, such as the transition density under discussion. To make a more specific comparison, we give the critical densities n_{cr}^{3D} in 3D case below [4]:

$$n_{cr}^{3D} = 2 \left(\frac{m_\alpha k_B T}{2\pi\hbar^2} \right)^{3/2} \frac{2}{\sqrt{\pi}} \int_0^\infty d\epsilon \, \frac{\sqrt{\epsilon}}{1 + \exp(\epsilon)} . \quad (14)$$

For electrons, it is about 10^{18} cm^{-3} and about 10^{19} cm^{-3} for holes at room temperature. Thus the difference in the transition density is explained from a numerical point of view. Next, the difference is scrutinized from the physical perspective. It is realized that reduced dimensionality makes it easier for fermionic particles to feel the presence of each other as compared to higher dimensions at the same temperature. The reason is simply that given the same de Broglie wavelength from the thermal energy, geometric restriction in lower dimension lead to higher filling efficiency to fully cover the volume or area. The fermionic gas becomes statistically degenerate when carrier density is high enough or temperature low enough such that particles, which are characterized by the de Broglie wavelength, overlap with each other. This means that the critical density is smaller than its counterpart in the bulk material and the lighter electrons has a lower critical density than the holes. As such, we explain the shift in the transition densities in 2D and 3D case. Other than D_{NN}, transitional behaviors in their density dependence also occurs for the other DCs in our quasi-2D case. It would be interesting to compare our quasi-2D results to 3D ones for other diffusion coefficients.

Last but not the least, we comment on the application aspect of the general two-component case where spatial charge separation occurs. Such a case can be implemented in type-II QW designs or by external modulation of the quantum confinement potential. It is interesting to note that even though screening effect is weakened in such a case, higher mobility could still be achieved by reduction in the e-h scattering. Furthermore, novel device designs could be conceptualized by the appearance of negative mobility for the minority carriers under certain conditions.

To conclude, we have presented the numerical results for the density-related diffusion coefficients in the general two-component case together with the results for all the diffusion coefficients under the single-component approximation for the *coupled diffusion model* which is developed for the hydrodynamic variables, *i.e.*, carrier density and temperature, of the electron-hole plasma within a semiconductor quantum well laser device. Also presented

are the carrier-LO phonon scattering and electron-hole scattering rates which are computed microscopically and used in the determination of the diffusion coefficients. Moreover, the diffusion coefficients are analyzed in the framework of free Fermi gas theory with the inclusion of many-body effects. In the general two-component case, it is found that the self- and mutual-diffusion coefficients are determined mainly by the free carrier contributions, but with appreciable many-body corrections near the critical density for the hole density coefficients. Carrier-LO phonon scattering is dominant at low density, but electron-hole scattering becomes important in determining their density dependence above the critical electron density. In the single-component case, it is found that many-body effects suppress the density coefficients but enhance the temperature coefficients. The modification is of the order of 10% and reaches a maximum of over 20% [10] for the density coefficients and keeps growing for the temperature coefficients in the parameter range

shown. However, the many-body effects play a minor role in determining the dependence of the coefficients on plasma density and temperature. The free carrier contributions are dominantly responsible for such dependence of the coefficients. Overall, temperature elevation enhances the diffusive capability or diffusion coefficients of carriers linearly, and such an enhancement grows with density. Simulation results based on the *coupled diffusion model* will be presented in a future work. Finally, we point out that the *model* in the general two-component case can be utilized as a design vehicle for novel devices.

Acknowledgments

[1] J. Li and C. Z. Ning, Phys. Rev. **A 65**, preceding article (2002).

[2] For Fermi gas theory, consult with any textbooks for solid state physics, such as Ref. [3]. For many-body corrections, refer to Ref. [6, 7, 11, 16, 17].

[3] N. W. Ashcroft and N. D. Mermin, *Solid State Physics* (Holt, Rinehart and Winston, New York, 1976).

[4] H. E. Ruda, J. Appl. Phys. **59**, 1120 (1986).

[5] L. P. Kadanoff and G. Baym, *Quantum Statistical Mechanics* (Addison-Wesley, Reading, 1989).

[6] S. W. Koch and H. Haug, *Theory of the Electrical and Optical Properties of Semiconductors* (World Scientific, Singapore, 1994), 3rd ed.

[7] W. W. Chow, S. W. Koch, and M. Sargent III, *Semiconductor Laser Physics* (Springer Verlag, Berlin, 1994).

[8] In our treatment of the Coulomb interaction within the electron-hole plasma model, the singularity in the potential can not be properly accounted for, which means that

no excitonic bound states are recovered, as far as carrier transport properties are concerned. As a result, the low density limit for many-body contributions is zero.

[9] J. R. Meyer, Phys. Rev. **B 21**, 1554 (1980).

[10] C. Z. Ning and J. Li, Phys. Rev. **B**: Rapid Communications, submitted (2002).

[11] H. Haug and S. W. Koch, Phys. Rev. **A 39**, 1887 (1989).

[12] S. Schmitt-Rink, C. Ell, and H. Haug, Phys. Rev. **B 33**, 1183 (1986).

[13] J. Li and C. Z. Ning, Proc. SPIE **3944**, 311 (2000).

[14] R. Zimmermann, Phys. Status Solidi B **146**, 371 (1988).

[15] P. T. Landsberg, Proc. IEEE **61**, 476 (1973).

[16] H. Haug and S. Schmitt-Rink, Prog. Quantum Electron. **9**, 3 (1984).

[17] R. Binder and S. W. Koch, Prog. Quantum Electron. **19**, 307 (1995).

[18] O. Hess and T. Kuhn, Phys. Rev. **A 54**, 3347 (1996).